

Characterization of $\text{Ln}_{0.8}\text{Sr}_{0.2}\text{CoO}_{3.5}$ (Ln=Gd, Nd, Pr, Sm, or Yb) as Cathode Materials for Low-Temperature SOFCs

Jung Woon Choi, Ju Hyun Kang, Han Ji Kim, and Kwang Soo Yoo[†]

Department of Materials Science and Engineering, University of Seoul, Seoul 130-743, Korea
(Received August 15, 2006; Accepted October 6, 2006)

ABSTRACT

Perovskites with nominal compositions $\text{Ln}_{0.8}\text{Sr}_{0.2}\text{CoO}_{3.5}$ (Ln=Gd, Nd, Pr, Sm, or Yb) were fabricated as cathode materials using a solid-state reaction method for low-temperature operating Solid-Oxide Fuel Cells (SOFCs). X-ray diffraction analysis and microstructure observation for the sintered samples were performed. The ac complex impedance was measured in the temperature range of 600-900°C in air and fitted with a Solartron ZView program. The crystal structure, microstructure, electrical conductivity, and polarization resistance of $\text{Ln}_{0.8}\text{Sr}_{0.2}\text{CoO}_{3.5}$ were characterized systematically.

Key words : SOFC, Cathode materials, Polarization resistance, Impedance, Porosity

1. Introduction

A fuel cell is a device that directly converts chemical energy into electrical energy. Solid-Oxide Fuel Cells (SOFCs) continue to attract interest as potentially reliable, durable, and inexpensive technology for generating electricity from hydrocarbon fuels. Compared with other fuel cells, fabrication of a SOFC is much simpler.¹⁾

SOFCs operating at temperatures near 1000°C are frequently studied due to the fact that they are environmentally friendly and can generate high levels of power efficiency. However, widely used interconnection materials, such as $\text{La}(\text{Sr})\text{CrO}_3$, account for much of the cell cost of high temperature SOFCs; thus commercialization of SOFCs has been hampered. If the operating temperature of a SOFC is reduced to less than 700°C, cheaper materials can be used in place of $\text{La}(\text{Sr})\text{CrO}_3$. The high power generation efficiency of SOFCs should be maintained at this low temperature, however. To achieve this, considerable efforts have been dedicated to reducing the ohmic loss of the electrolyte by fabricating a thin YSZ layer or by finding new materials with high ionic conductivity, such as Sc-stabilized zirconias.²⁾ It is important that the cathode materials have high electrical conductivity at a low temperature, adequate porosity for oxygen gas transportation, good compatibility with the electrolyte, and long-term stability. Recently, porous ceramic structures synthesized from perovskite oxides have been used as cathodes that provide low operating temperatures for SOFCs.³⁾ In these perovskites, substitution of a divalent cation for a trivalent cation results

mostly in electronic holes in air. At lower oxygen pressures, however, charge compensation is likely to be achieved through the formation of oxygen-ion vacancies. These oxygen vacancies provide a pathway for the oxide ions through the electrode material. Therefore, flux through the bulk electrode material is likely to increase. A high oxygen flux at modest overpotentials is expected to be an advantage of these materials for use as SOFC cathodes.⁴⁾

The objective of this study is to investigate the electrical properties of lanthanide cobaltite perovskite oxides as a function of the sintering conditions and composition. The electrical conductivity was evaluated using an impedance analyzer. The interfacial reaction and morphology between the cathode and the electrolyte were observed through Field Emission Scanning Electron Microscopy (FESEM). Following these analyses, the relationship between the polarization resistance and porosity was examined.

2. Experimental Procedure

As starting materials, Gd_2O_3 , Nd_2O_3 , Pr_2O_3 , Sm_2O_3 , Yb_2O_3 , SrCO_3 , and Co_2O_3 were used in this experiment. The powders were mixed in ethanol and milled for 48 h, after which the powders were pressed into pellets and calcined at 1000°C for 4 h. The cathode powders and the vehicle were mixed at a 75:25 weight ratio and ground to form a paste. 8-mol% YSZ was used as an electrolyte. The YSZ powder was pressed into a pellet and sintered at 1600°C for 4 h.

To study the electrical properties of the cathode materials, the slurry was screen-printed onto the YSZ electrolyte. The screen-printed samples were sintered at 1200°C for 3 h, as shown in Fig. 1. Following this procedure, Pt-paste was applied on the rear side of the YSZ electrolyte as the reference electrode and the counter electrode. The half-cells were

[†]Corresponding author : Kwang Soo Yoo
E-mail : ksyoo@uos.ac.kr
Tel : +82-2-2210-2514 Fax : +82-2-2215-5863

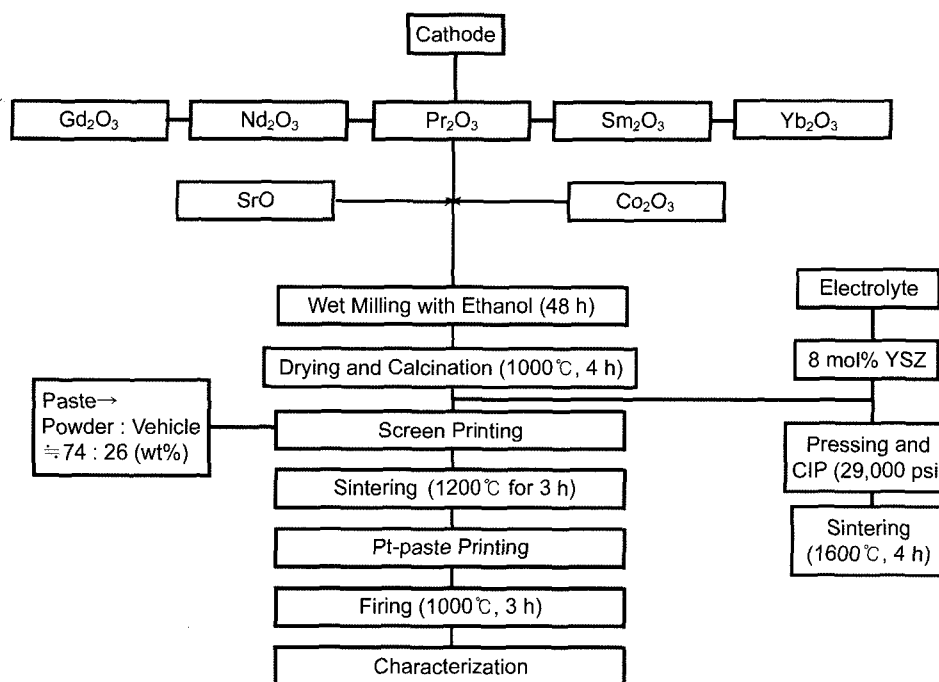


Fig. 1. Flow chart of the experimental procedure.

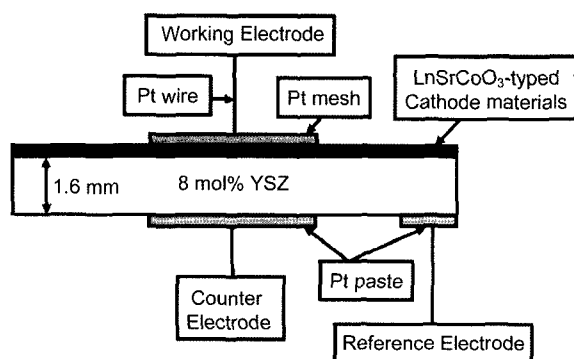


Fig. 2. Schematic diagram of the half-cell.

all formed as shown in Fig. 2. The YSZ electrolyte was approximately 1.6 mm in thickness. The interface between the cathode layer and the YSZ electrolyte was observed through the use of an FESEM (Hitachi 4300, Hitachi). The samples were mounted and polished before they were observed. Porosity was calculated using an Image Analyzer. Electrical properties were measured using an Impedance Analyzer (SI 1260, Solartron) and an Electrochemical Interface (SI 1287, Solartron). Measurements were taken without a DC bias and spectra were obtained within a frequency range of $3 \times 10^7 \sim 0.01$ Hz with an applied AC voltage amplitude of 10 mV. All of the samples were measured in a temperature range of 600–900°C.

3. Results and Discussion

3.1. Physical Properties

Fig. 3 shows XRD patterns of the lanthanide cobaltite

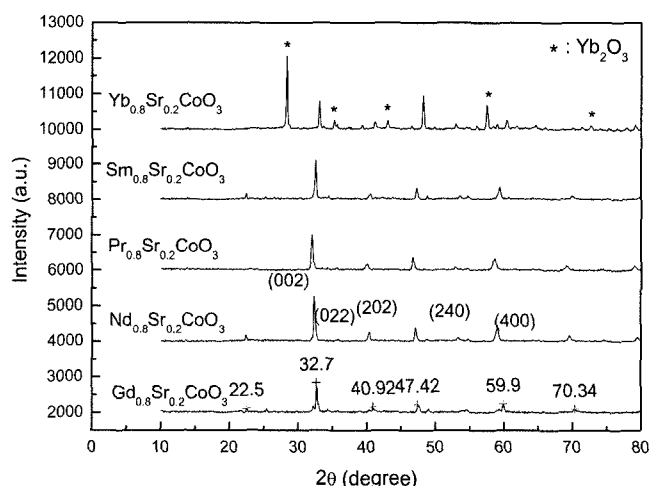


Fig. 3. X-ray diffraction data of the lanthanide cathode materials calcined at 1000°C for 4 h.

cathode materials after calcining at 1000°C for 4 h. From these results, the prepared cathode powders appeared to be single-phase without showing peaks from second phases except when Ln was Yb. In the case of the Yb-base cobaltite, peaks were detected from Yb_2O_3 along with those of $\text{Yb}_{0.8}\text{Sr}_{0.2}\text{CoO}_3$, a result that was also reported by James *et al.*²⁰⁾ It is postulated that for the $\text{Yb}_{0.8}\text{Sr}_{0.2}\text{CoO}_3$ cathode material, calcination at 1000°C for 4 h was insufficient for a single-phase synthesis, in contrast to the other cathode materials prepared.

In Fig. 4, the surface morphology of each cathode material is displayed. In Fig. 5, the interfaces between the cathode layer and the electrolyte are shown after cathode layer sin-

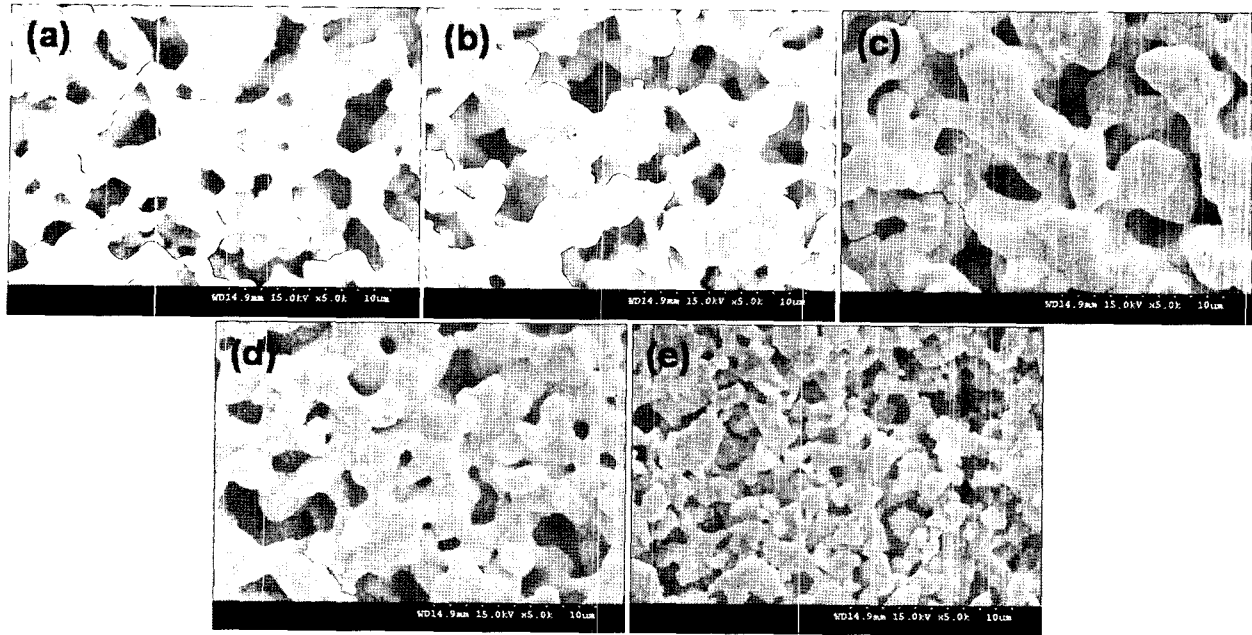


Fig. 4. Surface micrographs of the cathode material sintered at 1200°C for 3 h: (a) $Gd_{0.8}Sr_{0.2}CoO_{3.5}$, (b) $Nd_{0.8}Sr_{0.2}CoO_{3.5}$, (c) $Pr_{0.8}Sr_{0.2}CoO_{3.5}$, (d) $Sm_{0.8}Sr_{0.2}CoO_{3.5}$, and (e) $Yb_{0.8}Sr_{0.2}CoO_{3.5}$.

tering at 1200°C for 3 h. As seen from the SEM micrographs, the cathode layers on the YSZ electrolyte were very porous and the thickness of the cathode was approximately 15 μm . It was found that the cathode grains were well interconnected with high open porosity. The porosity was calculated using the image analyzer. With a range of 30% to 39%, the porosity is held to be sufficient for oxygen gas transport. The porosity of the $Sm_{0.8}Sr_{0.2}CoO_3$ was higher than that of the other samples. In addition, as shown in Fig. 5, the cath-

ode layers were relatively well adhered to the electrolyte. Consequently, it is thought adequate to secure the active sites for the oxygen reduction process in the cathode.

To investigate the long-term stability of the prepared cathode materials, samples were tested at 700°C for 100 h. Surface micrographs of these samples are shown in Fig. 6. All cathode layers continued to exhibit moderate adhesion to the YSZ electrolyte; however, compared with Fig. 4, it was observed that the connectivity of the cathode deteriorated

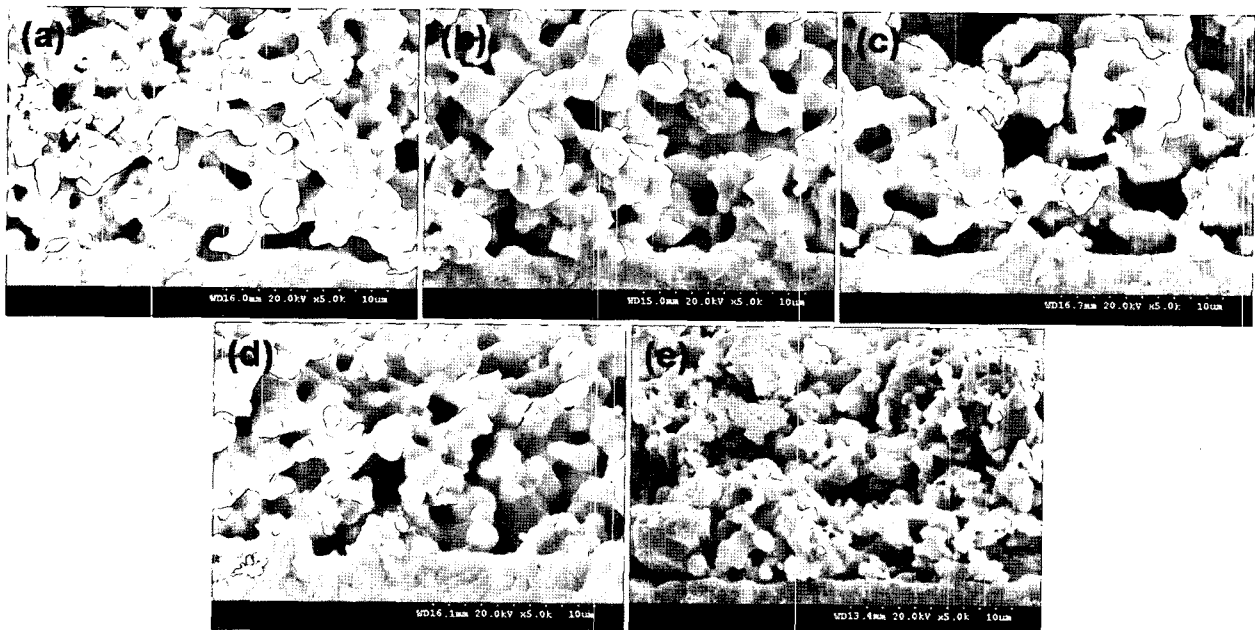


Fig. 5. Cross-sectional micrographs of the cathode material sintered at 1200°C for 3 h: (a) $Gd_{0.8}Sr_{0.2}CoO_{3.5}$, (b) $Nd_{0.8}Sr_{0.2}CoO_{3.5}$, (c) $Pr_{0.8}Sr_{0.2}CoO_{3.5}$, (d) $Sm_{0.8}Sr_{0.2}CoO_{3.5}$, and (e) $Yb_{0.8}Sr_{0.2}CoO_{3.5}$.

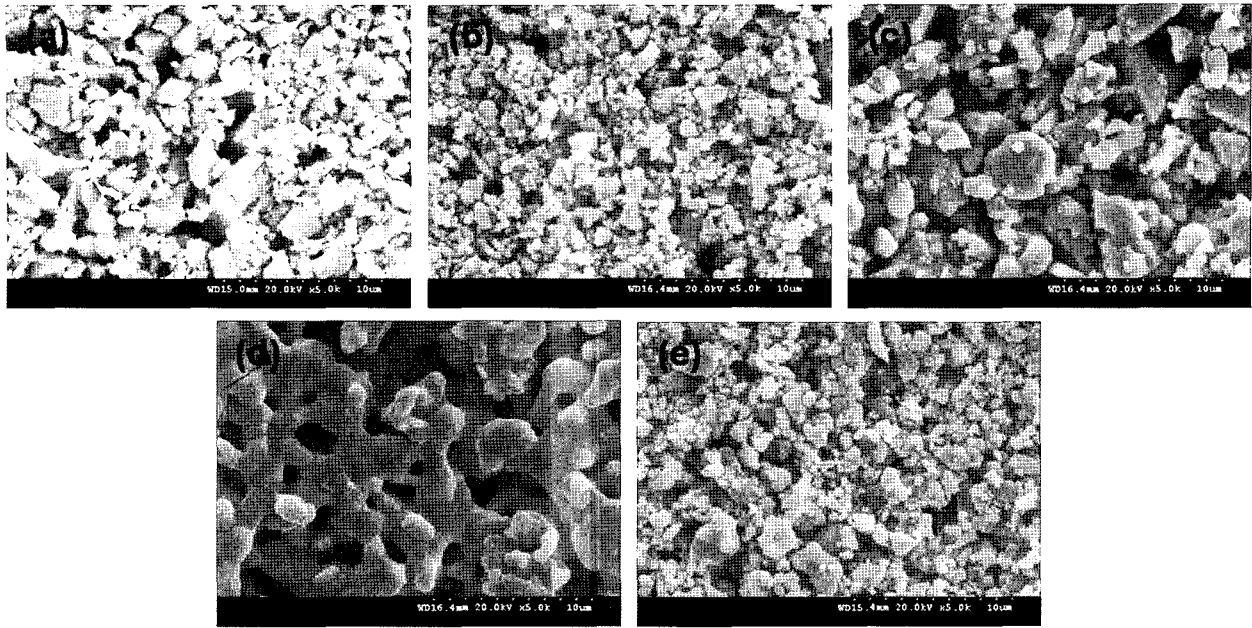


Fig. 6. Surface micrographs of the cathode materials tested at 700°C for 100 h: (a) $\text{Gd}_{0.8}\text{Sr}_{0.2}\text{CoO}_3$, (b) $\text{Nd}_{0.8}\text{Sr}_{0.2}\text{CoO}_3$, (c) $\text{Pr}_{0.8}\text{Sr}_{0.2}\text{CoO}_3$, (d) $\text{Sm}_{0.8}\text{Sr}_{0.2}\text{CoO}_3$, and (e) $\text{Yb}_{0.8}\text{Sr}_{0.2}\text{CoO}_{3-\delta}$.

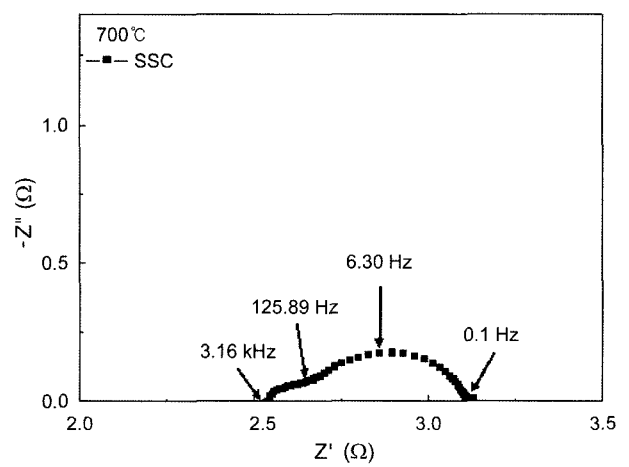
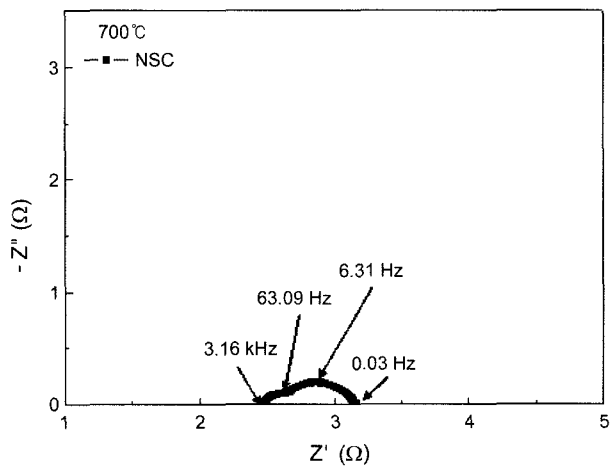
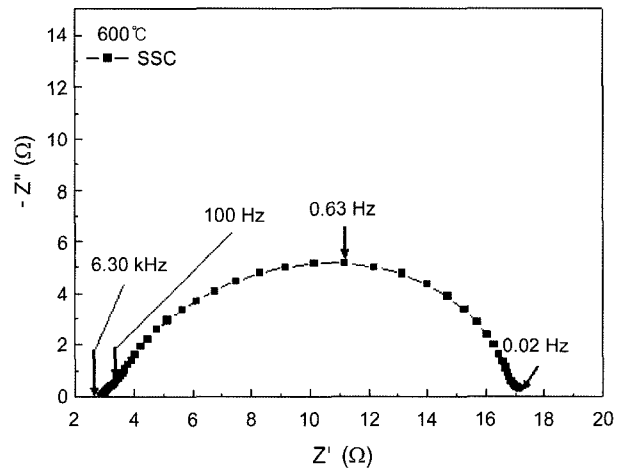
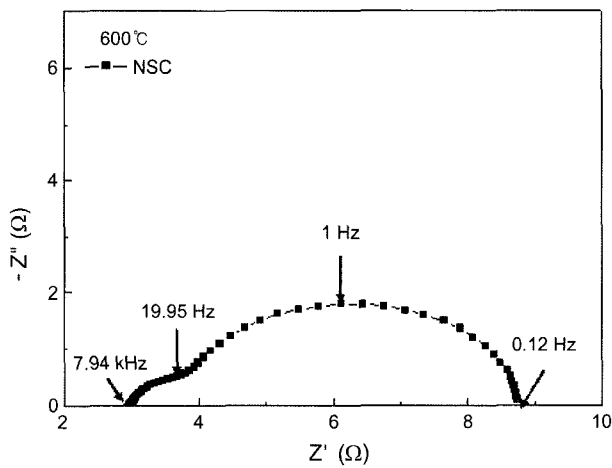


Fig. 7. Impedance spectra of the $\text{Nd}_{0.8}\text{Sr}_{0.2}\text{CoO}_3$ cathode material sintered at 1200°C for 3 h.

Fig. 8. Impedance spectra of the $\text{Sm}_{0.8}\text{Sr}_{0.2}\text{CoO}_3$ cathode material sintered at 1200°C for 3 h.

considerably after the test, with the exception of the $\text{Sm}_{0.8}\text{Sr}_{0.2}\text{CoO}_3$ cathode material.

3.2. Electrical Properties

In order to investigate the electrical properties of the samples, impedance measurements were carried out at 600°C, 700°C, 800°C, and 900°C. However, measurements of the Yb-base cobaltite were not taken, as a single-phase $\text{Yb}_{0.8}\text{Sr}_{0.2}\text{CoO}_3$ was not synthesized. In Figs. 7 and 8, selected impedance spectra of $\text{Nd}_{0.8}\text{Sr}_{0.2}\text{CoO}_3$ and $\text{Sm}_{0.8}\text{Sr}_{0.2}\text{CoO}_3$ at temperatures of 600°C and 700°C are presented. As shown in these figures, as the operating temperature increases, the polarization resistance values decrease due to the change in the electrode kinetics. The polarization resistance of the $\text{Nd}_{0.8}\text{Sr}_{0.2}\text{CoO}_3$ was $5.87 \Omega\text{cm}^2$ at 600°C, and at 700°C it was $0.81 \Omega\text{cm}^2$. From Fig. 8, the polarization resistance of $\text{Sm}_{0.8}\text{Sr}_{0.2}\text{CoO}_3$ was $13.8 \Omega\text{cm}^2$ at 600°C, while it was $0.56 \Omega\text{cm}^2$ at 700°C. Although the polarization resistance

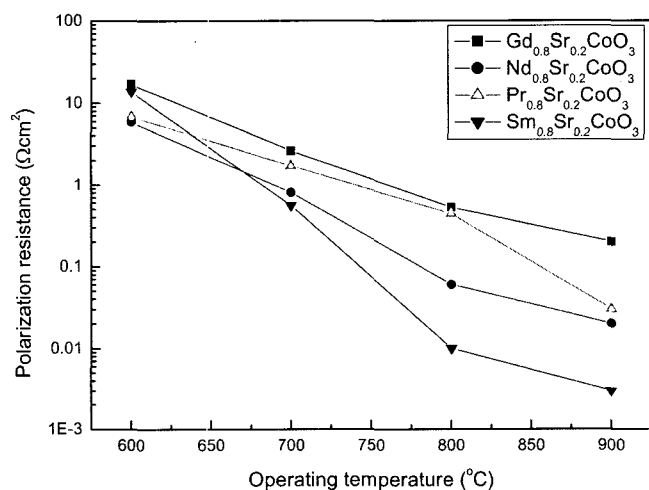


Fig. 9. Polarization resistance of the lanthanide cobaltite cathode materials.

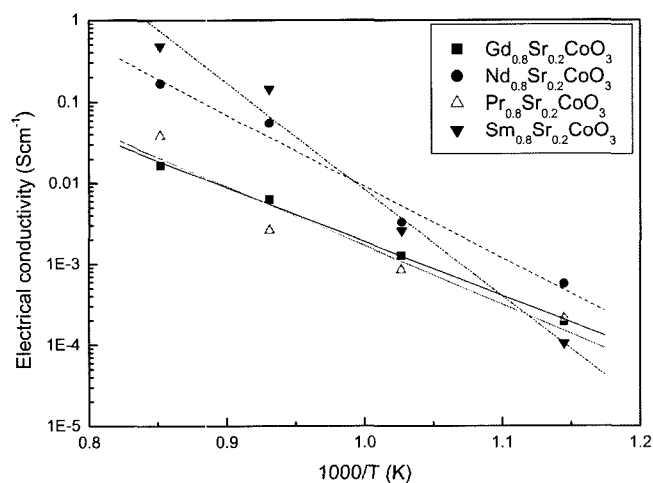


Fig. 10. Electrical conductivity of the lanthanide cobaltite cathode materials.

value of the $\text{Sm}_{0.8}\text{Sr}_{0.2}\text{CoO}_3$ cathode material was nearly twice that of $\text{Nd}_{0.8}\text{Sr}_{0.2}\text{CoO}_3$, the former was slightly lower than the latter at 700°C. The polarization resistance values for all of the cathode materials are depicted in Fig. 9, and the electrical conductivities are shown in Fig. 10. At temperatures over 700°C, compared with the other two materials, $\text{Nd}_{0.8}\text{Sr}_{0.2}\text{CoO}_3$ and $\text{Sm}_{0.8}\text{Sr}_{0.2}\text{CoO}_3$ exhibited lower polarization resistance values and higher electrical conductivities. At 700°C, the electrical conductivities of $\text{Nd}_{0.8}\text{Sr}_{0.2}\text{CoO}_3$ and $\text{Sm}_{0.8}\text{Sr}_{0.2}\text{CoO}_3$ were similar, at 0.003 Scm^{-1} and 0.002 Scm^{-1} , respectively.

It is thought that the superior performance of $\text{Sm}_{0.8}\text{Sr}_{0.2}\text{CoO}_3$ originates from the higher porosity relative to the other materials with the identical preparation methods described in the previous section. The porosity is most important in decreasing the polarization resistance, as the area of the Three-Phase Boundary (TPB) consisting of the cathode, electrolyte, and pore phases, would increase with open porosity; moreover, there is the benefit of the reduction of the polarization resistance. In addition, considering the microstructural change at 700°C shown in Fig. 6, it is believed that $\text{Sm}_{0.8}\text{Sr}_{0.2}\text{CoO}_3$ is likely a better cathode material at 700°C compared to $\text{Nd}_{0.8}\text{Sr}_{0.2}\text{CoO}_3$, as the former showed a more stable structure than did the latter at 700°C. At 800 and 900°C, $\text{Sm}_{0.8}\text{Sr}_{0.2}\text{CoO}_3$ showed significantly lower polarization resistance values and higher electrical conductivities than the other materials. The mechanism for such improvements is not yet well understood and requires further research.

4. Conclusions

Perovskite materials with nominal compositions $\text{Ln}_{0.8}\text{Sr}_{0.2}\text{CoO}_{3.5}$ ($\text{Ln}=\text{Gd}, \text{Nd}, \text{Pr}, \text{Sm}, \text{or Yb}$) were fabricated as cathode materials for low-temperature operating Solid Oxide Fuel Cells (SOFCs). Their physical and electrical properties were then investigated. All samples sintered for 3 h at 1200°C were observed to have a sufficient porosity for cathode materials, but $\text{Sm}_{0.8}\text{Sr}_{0.2}\text{CoO}_3$ showed the highest porosity. The microstructure of $\text{Sm}_{0.8}\text{Sr}_{0.2}\text{CoO}_3$ did not change after a long-term stability test at 700°C. In contrast to the other candidates tested. Impedance analyses were performed on half-cells fabricated with $\text{Ln}_{0.8}\text{Sr}_{0.2}\text{CoO}_{3.5}$ on a YSZ electrolyte, and the cell with the $\text{Nd}_{0.8}\text{Sr}_{0.2}\text{CoO}_{3.5}$ cathode layer showed a polarization resistance of $5.87 \Omega\text{cm}^2$ at 600°C, which was the lowest value at this temperature. However, at an operating temperature of 700°C, $\text{Sm}_{0.8}\text{Sr}_{0.2}\text{CoO}_{3.5}$ showed a lower polarization resistance relative to the other cathode materials. Considering both the physical and electrical properties, it is believed that the $\text{Sm}_{0.8}\text{Sr}_{0.2}\text{CoO}_3$ cathode material is likely a suitable choice for low-temperature SOFCs.

Acknowledgment

This work was supported by the Core Technology Devel-

opment Program for Fuel Cells of the Ministry of Commerce, Industry and Energy of Korea.

REFERENCES

1. J. M. Ralph, A. C. Schoeler, and M. Krimplet, "Materials for Lower Temperature Solid Oxide Fuel Cells," *J. Mater. Sci.* **36** 1161-72 (2001).
2. R. Chiba, F. Yoshimura, and Y. Sakurai, "Properties of $\text{La}_{1-y}\text{Sr}_y\text{Ni}_{1-x}\text{Fe}_x\text{O}_3$ as a Cathode Material for a Low-Temperature Operating SOFC," *Solid State Ionics*, **152-153** 575-82 (2002).
3. M. T. Colmer, B. C. H. Steels, and J. A. Kilner, "Structural and Electrochemical Properties of the $\text{Sr}_{0.8}\text{Ce}_{0.2}\text{Fe}_{0.7}\text{Co}_{0.3}\text{O}_{3.5}$ Perovskite as Cathode Material for ITSOFCs," *Solid State Ionics*, **147** 41-8 (2002).
4. E. Maguire, B. Gharbage, F. A. B. Marques, and J. A. Labrincha, "Cathode Materials for Intermediate Temperature SOFCs," *Solid State Ionics*, **127** 329-35 (2000).
5. C. R. Xia, W. Rauch, W. Wellborn, and M. L. Liu, "Functionally Graded Cathodes for Honeycomb Solid Oxide Fuel Cells," *Electrochem. Solid State Lett.*, **5** A217-20 (2002).
6. C. R. Xia and M. L. Liu, "Novel Cathodes for Low-Temperature Solid Oxide Fuel Cells," *Adv. Mater.*, **14** 521-23 (2002).
7. C. Y. Huang and T. J. Huang, "Effect of Co Substitution for Mn on $\text{Y}_{1-x}\text{Sr}_x\text{MnO}_3$ Properties for SOFC Cathode Material," *J. Mater. Sci.*, **37** 4581-87 (2002).
8. S. R. Wang, T. Kato, S. Nagata, T. Honda, T. Kaneko, N. Iwashita, and M. Dokiya, "Performance of a $\text{La}_{0.6}\text{Sr}_{0.4}\text{Co}_{0.8}\text{Fe}_{0.2}\text{O}_3\text{-Ce}_{0.8}\text{Gd}_{0.2}\text{O}_{1.9}\text{-Ag}$ Cathode for Ceria Electrolyte SOFCs," *Solid State Ionics*, **146** 203-10 (2002).
9. P. Holtappels and C. Bagger, "Fabrication and Performance of Advanced Multi-Layer SOFC Cathodes," *J. Eur. Ceram. Soc.*, **15** 41-8 (2002).
10. S. P. Jiang, Y. J. Leng, S. H. Chan, and K. A. Khor, "Development of (La,Sr)MnO₃-Based Cathodes for Intermediate Temperatures Solid Oxide Fuel Cells," *Electrochem Solid State Lett.*, **6** A67-A70 (2003).
11. S. Hashimoto, K. Kammer, P. H. Larsen, F. W. Poulsen, and M. Mogensen, "A Study of $\text{Pr}_{0.7}\text{Sr}_{0.3}\text{Fe}_{1-x}\text{Ni}_x\text{O}_{3.5}$ as a Cathode Material for SOFCs with Intermediate Operating Temperature," *Solid State Ionics*, **176** 1013-20 (2005).
12. Y. Liu, W. Rauch, S. Zha, and M. L. Liu, "Fabrication of $\text{Sm}_{0.5}\text{Sr}_{0.5}\text{CoO}_{3.5}\text{-Sm}_{0.1}\text{Ce}_{0.9}\text{O}_{2.8}$ Cathodes for Solid Oxide Fuel Cells Using Combustion CVD," *Solid State Ionics*, **166** 261-68 (2004).
13. A. Esquirol, N. P. Brandon, J. A. Kilner, and M. Mogensen, "Electrochemical Characterization of $\text{La}_{0.6}\text{Sr}_{0.4}\text{Co}_{0.2}\text{Fe}_{0.8}\text{O}_3$ Cathodes for Intermediate-Temperature SOFCs," *J. Electrochem. Soc.*, **151** A1847-55 (2004).
14. L. Qiu, T. Ichikawa, A. Hirano, N. Imanishi, and Y. Takeda, " $\text{Ln}_{1-x}\text{Sr}_x\text{Co}_{1-y}\text{Fe}_y\text{O}_{3.5}$ (Ln = Pr, Nd, Gd; x = 0.2, 0.3) for the Electrodes of Solid Oxide Fuel Cells," *Solid State Ionics*, **158** 55-65 (2003).
15. R. Chiba, F. Yoshimura, Y. Sakurai, Y. Tabata, and M. Arakawa, "A Study of Cathode Materials for Intermediate Temperature SOFCs Prepared by the Sol-Gel Method," *Solid State Ionics*, **175** 23-7 (2004).
16. H. Zhao, L. Huo, and S. Gao, "Electrochemical Properties of LSM-CBO Composite Cathode," *J. Power Sources*, **125** 149-54 (2004).
17. W. X. Chen, T. L. Wen, H. W. Nie, and R. Zheng, "Study of $\text{Ln}_{0.6}\text{Sr}_{0.4}\text{Co}_{0.8}\text{Mn}_{0.2}\text{O}_{3.5}$ (Ln = La, Gd, Sm or Nd) as the Cathode Materials for Intermediate Temperature SOFC," *Mater. Res. Bull.*, **38** 1319-28 (2003).
18. Z. P. Shao and S. M. Haile, "A High-Performance Cathode for the Next Generation of Solid-Oxide Fuel Cells," *Nature*, **431** 170-73 (2004).
19. N. P. Brandon, S. Skinner, and B. C. H. Steele, "Recent Advances in Materials for Fuel Cells," *Ann. Rev. Mater. Res.*, **33** 183-213 (2003).
20. M. James, D. Cassidy, D. J. Goossens, and R. L. Withers, "The Phase Diagram and Tetragonal Superstructures of the Rare Earth Cobaltate Phases $\text{Ln}_{1-x}\text{Sr}_x\text{CoO}_{3.5}$ (Ln = La^{3+} , Pr^{3+} , Nd^{3+} , Sm^{3+} , Gd^{3+} , Y^{3+} , Ho^{3+} , Dy^{3+} , Er^{3+} , Tm^{3+} , and Yb^{3+})," *J. Solid State Chem.*, **177** 1886-95 (2004).